

Structure–activity studies of rapamycin analogs: evidence that the C-7 methoxy group is part of the effector domain and positioned at the FKBP12–FRAP interface

Juan I Luengo^{1*}, Dennis S Yamashita¹, Damien Dunnington², Arda Konialian Beck¹, Leonard W Rozamus¹, Hwa-Kwo Yen¹, Mary J Bossard¹, Mark A Levy¹, Annalisa Hand², Tonie Newman-Tarr², Alison Badger², Leo Faucette³, Randall K Johnson³, Karla D'Alessio⁴, Terence Porter⁴, Arthur YL Shu⁵, Richard Heys⁵, Jungwon Choi⁶, Polongpon Kongsaree⁶, Jon Clardy^{6†} and Dennis A Holt^{1*‡}

Departments of ¹Medicinal Chemistry, ²Cellular Biochemistry, ³Biomolecular Discovery, ⁴Protein Biochemistry and ⁵Synthetic Chemistry, SmithKline Beecham Pharmaceuticals, King of Prussia, PA 19406, USA and ⁶Department of Chemistry, Cornell University, Ithaca, NY 14853-1301, USA

Background: Rapamycin is an immunosuppressant natural product, which blocks T-cell mitogenesis and yeast proliferation. In the cytoplasm, rapamycin binds to the immunophilin FKBP12 and the complex of these two molecules binds to a recently discovered protein, FRAP. The rapamycin molecule has two functional domains, defined by their interaction with FKBP12 (binding domain) or with FRAP (effector domain). We previously showed that the allylic methoxy group at C-7 of rapamycin could be replaced by a variety of different substituents. We set out to examine the effects of such substitutions on FKBP12 binding and on biological activity.

Results: Rapamycin C-7-modified analogs of both *R* and *S* configurations were shown to have high affinities for FKBP12, yet these congeners displayed a wide range of

potencies in splenocyte and yeast proliferation assays. The X-ray crystal structures of four rapamycin analogs in complexes with FKBP12 were determined and revealed that protein and ligand backbone conformations were essentially the same as those observed for the parent rapamycin–FKBP12 complex and that the C-7 group remained exposed to solvent. We then prepared a rapamycin analog with a photoreactive functionality as part of the C-7 substituent. This compound specifically labeled, in an FKBP12-dependent manner, a protein of ~250 kDa, which comigrates with recombinant FRAP.

Conclusions: We conclude that the C-7 methoxy group of rapamycin is part of the effector domain. In the ternary complex, this group is situated in close proximity to FRAP, at the interface between FRAP and FKBP12.

Chemistry & Biology July 1995, 2:471–481

Key words: atomic model, FKBP, photoaffinity label, rapamycin, structure–activity relationships, X-ray crystal structure

Introduction

Rapamycin (compound **1**, Fig. 1) is an extraordinary natural product which has attracted considerable interest and study in disciplines spanning the fields of chemistry and biology [1,2]. This metabolite from *Streptomyces* was first isolated and characterized as an antimicrobial antitumor agent in 1975. More recently, rapamycin has received attention as an extremely potent immunosuppressant and is currently undergoing clinical investigation for the prevention of transplant rejection. Perhaps the most remarkable fact about rapamycin is that, like its pharmacological cousins FK506 and cyclosporin A, it falls into a small but undoubtedly expanding group of small organic molecules that function by inducing specific protein–protein heterodimerization [3].

Rapamycin and FK506 (compound **2** in Fig. 1) both bind with high affinity to the immunophilin FKBP12 and inhibit its rotamase (peptidyl prolyl *cis*–*trans* isomerase) activity [4]. Inhibition of this activity, however, is

only indirectly related to the cellular effects of these immunosuppressive drugs [5,6]. The FKBP12–rapamycin and FKBP12–FK506 complexes bind to secondary target proteins, apparently disrupting their critical physiological functions. The protein target for the FKBP12–FK506 complex is the calcium-dependent phosphatase calcineurin, an essential component of the intracellular signaling pathway linking the transmembrane T-cell receptor to the transcription of genes required early in activation such as IL-2 [7]. The structurally unrelated immunosuppressant cyclosporin A (CsA) binds with high affinity to another family of immunophilin proteins, the cyclophilins (CyPs), which are structurally unrelated to the FKBP12. The resulting CyP–CsA complex, however, also binds to calcineurin, inhibiting its protein phosphatase activity. By inhibiting the reactivity of calcineurin, both CyP and FK506 block calcium-dependent T-cell activation events, such as the response to the interaction of the T-cell receptor with its ligand. In contrast, the FKBP12–rapamycin complex does not bind to calcineurin, nor does

*Corresponding authors. †Corresponding author for X-ray structure determination. ‡Present address: ARIAD Pharmaceuticals, 26 Landsdowne Street, Cambridge, MA 02139, USA.

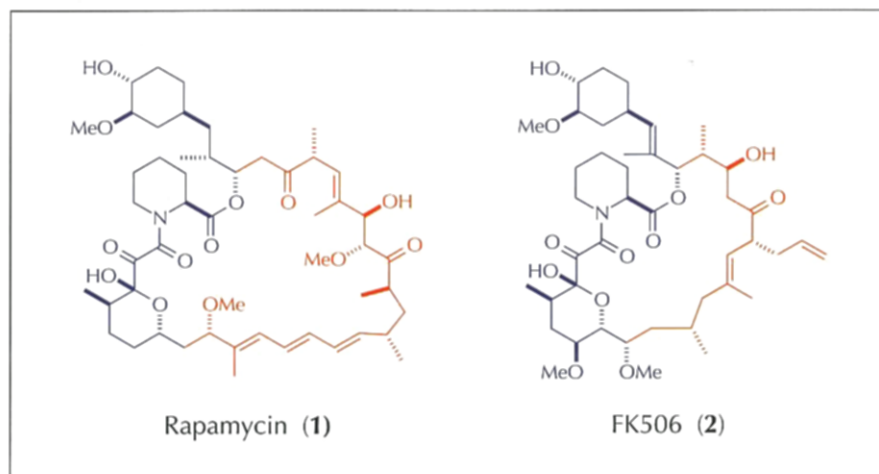


Fig. 1. Structures of the immunosuppressive FKBP12 ligands rapamycin (compound 1) and FK506 (compound 2) showing their common binding domains (blue) and distinct effector domains (red).

rapamycin block calcium-dependent signaling or its result, entry into the cell cycle. Instead, rapamycin has been shown to block T-cell responses to IL-2, preventing the activation of p70^{S6} kinase (p70^{S6K}) and cyclin-dependent kinases, and inhibiting the progression of the cell cycle at the G1 phase [2]. Very recently, the target of the rapamycin–FKBP12 complex has been reported as a 289-kDa protein (FRAP, RAFT1, RAPT1, SEP [8–11]), which is thought to be a lipid kinase, and has homology to the yeast TOR/DRR gene products [12,13]. The role of FRAP in activating p70^{S6K} and cyclin-dependent kinases has yet to be elucidated.

X-ray crystal structures of the FKBP12–FK506 and FKBP12–rapamycin complexes have been determined at atomic resolution, revealing that the ligands have two functional domains, a binding domain and an effector domain [14]. The common domains of the natural products (blue regions, centered on the α -keto piperolate, in Fig. 1) bind in an identical fashion within a hydrophobic pocket of FKBP12, whereas the dissimilar effector domains (red regions in Fig. 1) protrude from the protein and contribute to unique composite binding surfaces. In the complex with FK506, two regions in FKBP12, the 40s and 80s loops (Fig. 2), have been shown to be required for recognition of the bimolecular complex by calcineurin, suggesting that these two loops, together with a portion of the FK506 macrocyclic ring, might directly interact with calcineurin [15,16]. Although no information is yet available on the determinants for recognition of the FKBP12–rapamycin complex by FRAP, examination of the crystal structure of this complex reveals that an extended hydrophobic surface is formed by the same two loops of the protein and the trienyl region of rapamycin macrocycle. As shown in Fig. 2, this composite surface is slightly convex; it might form an important part of the surface recognized by FRAP. The crystal structure also shows that the C-7 methoxy group in rapamycin makes no direct contact with FKBP12. The position of this group, in the middle of this composite surface (roughly equidistant from the 40s and 80s loops, Fig. 2), indicates that it may be important in the function of the effector domain.

During the course of our exploration of the chemistry of rapamycin, we discovered that the C-7 methoxy group readily undergoes heterolytic cleavage under acid catalysis [17]. Ionization of the allylic methoxyl is assisted by the neighboring 1,3,5-conjugated triene, which presumably stabilizes the carbocation at C-7 by conjugation (structure 3 in Fig. 3). Under the acidic reaction conditions in which it is generated, this ambident electrophilic intermediate can be treated with nucleophiles, which, in most cases, are captured exclusively at the C-7 terminus. We have probed the role of the C-7 methoxyl in the effector domain of rapamycin using this chemistry and generated a series of analogs, including a photoreactive affinity agent. In this report, we describe structure–activity relationships for a limited number of analogs and show that the C-7 photoaffinity reagent labels a protein of similar electrophoretic mobility to FRAP. The results suggest that the C-7 position of rapamycin is part of its effector domain.

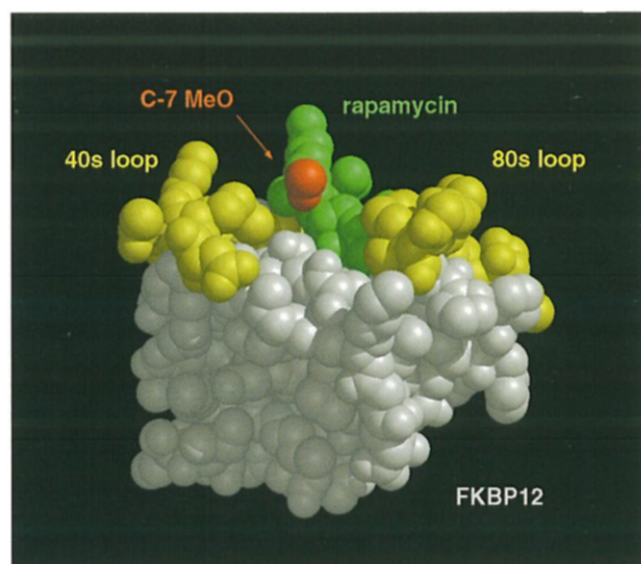


Fig. 2. View of the crystal structure of the FKBP12–rapamycin complex [14]. The 40s and 80s loops are shown in yellow, the rest of the protein in white; rapamycin is shown in green, with the C-7 methoxy group in red.

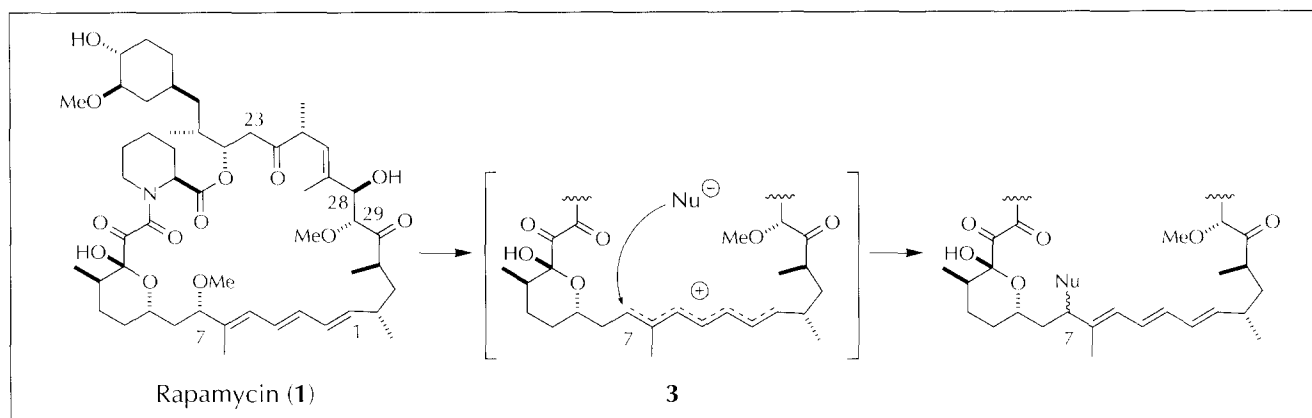


Fig. 3. The S_N1 reaction at rapamycin C-7. The 7-MeO group can be replaced by a variety of nucleophiles (ROH, RCO_2H , RSH, ArNH_2 , RSO_2NH_2 , electron-rich aromatics, Et_3SiH) by catalysis with trifluoroacetic acid (TFA) (CH_2Cl_2 , -40°C) or *p*-toluene sulfonic acid (*p*-TsOH) (ROH, room temperature).

Results and discussion

Synthesis of rapamycin C-7 analogs

The process of S_N1 substitution of the C-7 methoxy group of rapamycin was found to be of broad scope and was effected with a variety of catalysts (both protic and Lewis acids) and nucleophilic agents (e.g., alcohols, carboxylic acids, thiols, thioacids, aromatic amines, carbamates, sulfonamides, electron-rich aromatics, and allyl silanes). Most analogs were obtained by reaction with trifluoroacetic acid at low temperature (-40°C , CH_2Cl_2) in the presence of the nucleophile, except the C-7 ethers, which were more conveniently prepared by solvolysis of rapamycin in the appropriate alcohol catalyzed by *p*-toluenesulfonic acid. Nearly all reactions provided mixtures of C-7 diastereomeric products which were readily separable by chromatography. In addition, silane-based hydride reducing reagents provided 7-demethoxyrapamycin (compound **12**; Table 1) and in a process involving a related stabilized C-7 carbocation, treatment of rapamycin with quinone oxidants yielded 7-demethoxy-7-oxorapamycin (compound **13**). Products of elimination were never isolated from reactions of rapamycin with the above acids, even in the absence of added nucleophiles; however treatment of rapamycin with lithium perchlorate in diethyl ether resulted in efficient elimination of the C-7 methoxy group to generate stereospecifically the all-*trans* 1,3,5,7-tetraene derivative.

Effects of C-7 modification on FKBP12 binding

The intracellular activity of rapamycin is dependent upon its affinity for FKBP12 as well as the affinity of the resulting FKBP12–rapamycin complex for FRAP. As a close approximation of FKBP12 affinity, inhibition of rotamase catalytic activity (reported throughout as apparent inhibition constants, $K_{i,\text{app}}$) was determined for the rapamycin congeners using the standard chymotrypsin-coupled assay [18].

Representative examples of over 100 analogs which have been synthesized and assayed are shown in Table 1. A complete account of structure–activity relationships for this class will be reported separately. The great majority of analogs studied exhibited high affinity for FKBP12,

typically displaying rotamase inhibition within the same order of magnitude as rapamycin ($K_{i,\text{app}} = 0.5\text{ nM}$). This is not unexpected, since all the analogs share the same binding domain, which is identical to the one in rapamycin. However, some analogs, exemplified by compounds **8b** and **13**, had significantly weaker binding ($K_{i,\text{app}} = 25\text{--}40\text{ nM}$). In general, compounds of lower affinity contain bulkier hydrophobic C-7 substituents, perhaps reflecting greater C-7 steric demand or the possibility that the lipophilic C-7 substituent becomes more solvent-exposed upon binding to FKBP. In the case of compound **13**, the conjugated ketone at C-7 could have a long range effect on the conformation of the binding domain by the additional constraint imposed on the macrocyclic ring.

Spectroscopic analysis by NMR indicated that in non-aqueous solution, the analogs exist mainly as the *trans* amide rotamers, but adopt two distinct macrocyclic conformations depending on the specific configuration at C-7 (see Fig. 4). The conformation of all the 7-(*S*) epimers (compounds **5a–11a**) is identical to the one of rapamycin, but quite different from the one adopted by the 7-(*R*) epimers (compounds **5b–11b**), as indicated by the chemical shifts (both ^1H and ^{13}C NMR) and $^{1,3}J$ vicinal coupling constants of macrocyclic protons. Nevertheless, both C-7 stereochemistries seem to be well tolerated by FKBP12, since typically, K_i differences between epimeric pairs were less than four- to five-fold.

Effects of C-7 modification on inhibition of splenocyte and yeast proliferation

Suppression of mitogen-activated lymphocyte or splenocyte proliferation (as measured by uptake of thymidine) has in one of several forms become a standard *in vitro* measure of immunosuppressant activity. The potencies of FK506 and, more recently, rapamycin congeners in this model have been correlated with their FKBP12 affinities and with their abilities as FKBP12 complexes to bind to calcineurin [19] or FRAP [8]. Similarly, the abilities of FK506 and rapamycin to arrest yeast growth in S and G1 phases have been shown to be dependent upon FKBP12

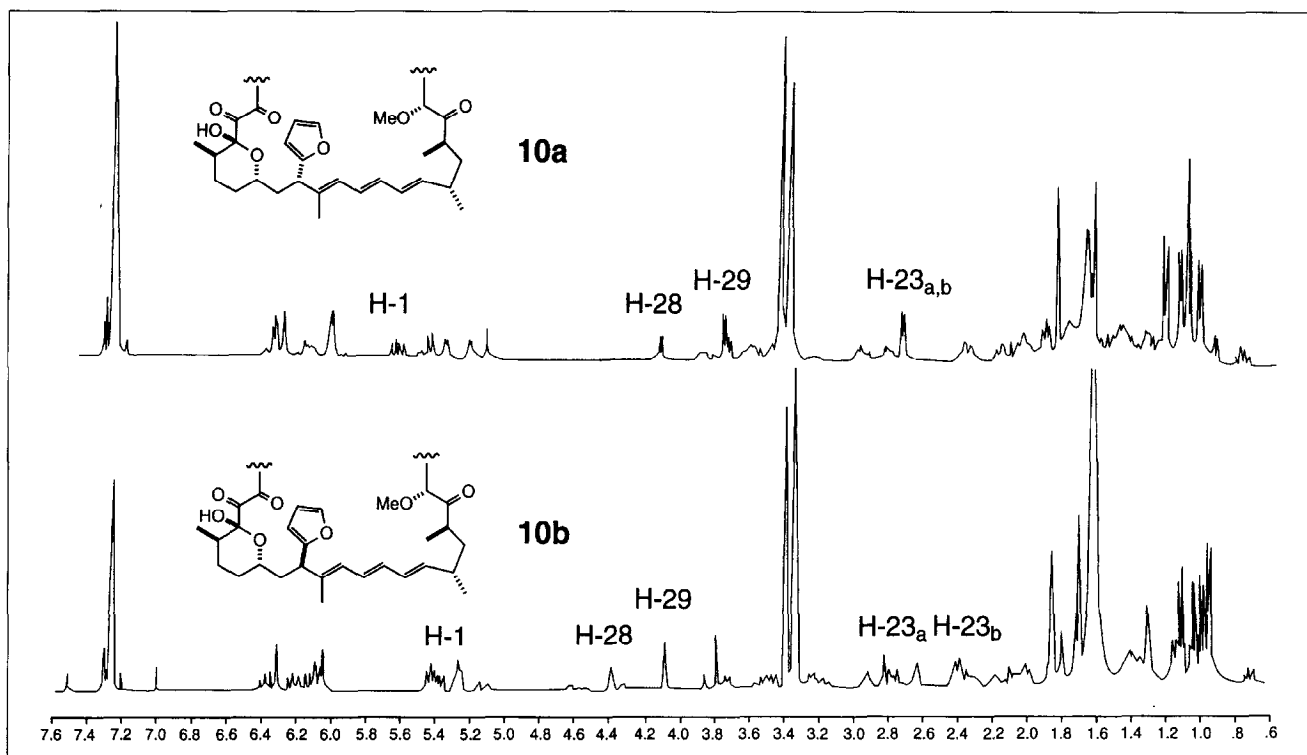


Fig. 4. Determination of the conformations of compounds **10a** and **10b**. 400-MHz ¹H NMR spectra of compound **10a** (top) and compound **10b** (bottom). The configuration at C-7 could be determined by ¹H and ¹³C NMR analysis, since the spectra of each epimeric pair were very different from each other, but almost identical within the same epimeric series.

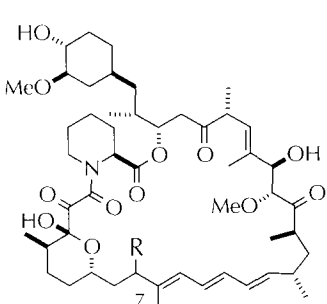
[20] as well as calcineurin [21] and the FRAP-related DRR/TOR gene products [12]. We therefore used both a mouse splenocyte mitogenesis assay and a high-flux yeast-based assay system to study the biological profiles of the rapamycin derivatives reported here.

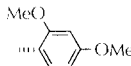
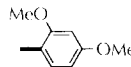
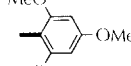
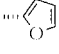
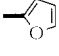
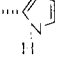
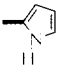
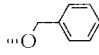
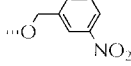
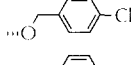
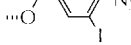
Remarkably, modification of the C-7 position of rapamycin resulted in a wide range of biological activities and, significantly, a divergence with respect to FKBP12 binding. Rapamycin shows an IC_{50} in the splenocyte assay of 1 nM and an IC_{50} in the yeast assay of 7 nM (Table 1). The C-7 methoxy group does not appear to be important in the activity of rapamycin since its removal, for example in 7-demethoxyrapamycin (compound **12**), leads to an analog with an identical biological profile to rapamycin itself. In general, analogs with small groups at C-7 (e.g. compounds **6a** and **6b**) showed activities in both splenocyte and yeast assays comparable to those of rapamycin, regardless of the C-7 configuration. Some analogs that retained high FKBP12 affinity showed markedly decreased activity in the cellular assays (e.g., compounds **7a**, **9**), suggesting that their C-7 substituents prevented binding of the associated FKBP12 complex to FRAP. Intermediate between these extremes, some analogs possessed measurable, yet less potent (10 to 100-fold weaker than rapamycin) yeast and splenocyte activities. Some analogs also showed a divergence of potencies between the yeast and splenocyte assays (e.g., compounds **5b**, **7a**, **10b**), presumably due to heterologies in the FRAP and TOR proteins. Differences in binding of an FK506-analog/FKBP

complex to yeast and mammalian calcineurins have similarly been reported [22]. Although it is possible that these analogs differ in their ability to penetrate cells, the results of these studies appear consistent with the notion that the C-7 methoxy substituent comprises part of the rapamycin effector domain, closely approaching, if not contacting, FRAP in the ternary complex, although it is not essential for binding. There seem to be some constraints associated with the size of the C-7 substituent, so that bulky, rigid groups, such as the 7(*R*)-1',3',5'-trimethoxybenzene ring in **9**, interfere with the binding interaction between FRAP and the FKBP12-rapamycin complex. To provide more direct evidence for the notion that the C-7 substituents are in close proximity to FRAP, we designed and synthesized a C-7 radio-photoaffinity derivative of rapamycin.

Photoaffinity labeling of a putative FKBP12-rapamycin binding protein

The hypothesized positioning of the rapamycin C-7 substituent at the interface between FKBP12 and the rapamycin target (recently identified as FRAP) and the tolerance to a variety of C-7 substitutions, suggested that an appropriate C-7 substituent could be used to carry a reactive functional group that could specifically tag the target partner protein. Indeed, a benzyloxy substituent appeared to be ideal since the corresponding benzyl ether (compound **14a**, Table 1) retained potent biological activity and the aromatic ring in **14a** could tolerate small *meta* and *para* substituents, such as those in compounds **15a** and **16a**, without a large decrease in activity.

Table 1. Biological activities of rapamycin C-7 analogs.^a


R	Compound	FKBP K _i (nM)	T Cell IC ₅₀ (nM)	Yeast IC ₁₂ (nM)
---OMe	1	0.6	1	7
—OMe	4	1	30	20
---OEt	5a	3.5	10	10
—OEt	5b	4	200	15
---SMe	6a	1	4	4
—SMe	6b	1	4	4
---NHCO ₂ Me	7a	4.5	>10000	170
—NHCO ₂ Me	7b	3.7	2500	220
	8a	9	1000	225
	8b	38	>1000	400
	9	7	>1000	>10000
	10a	3	20	12.5
	10b	6	20	3
	11a	10	11	28
	11b	1.5	70	28
—H	12	1	2	8
—O	13	29	300	210
	14a	5	6	6
	15a	7	50	20
	16a	1	45	6
	17a	30	90	60

^aC-7 configuration is 7-(S) (same as rapamycin) for **Xa** and 7-(R) for **Xb**.

We therefore prepared a compound with suitable functional groups for a radiophotoaffinity label (compound **17a**), containing a 4-azido-3-¹²⁵I]benzyloxy group at C-7. The synthesis of **17a** was accomplished starting with the iodination of 4-amino methyl benzoate (compound **18**) as shown in Fig. 5. After conversion of the amine to the azide, the ester was reduced to provide the required 4-azido-3-iodo benzyl alcohol (compound **19**). A route was devised to incorporate ¹²⁵I at a late stage, to minimize the number of radioactive synthetic intermediates. The iodo alcohol **19** was therefore subjected to palladium-catalyzed stannylation to give the arylstannane **20**. Reaction of **19** and rapamycin with *p*-TsOH in CH₂Cl₂ at room temperature produced a 1:1 mixture of separable C-7 epimers **17a** and **17b** in 66 % yield (Fig. 5). Incorporation of compound **20** into the C-7 position of rapamycin produced compound **21a** in lower yield due to competing protodestannylation (14 % yield, epimer **21b** not isolated). Exchange of the stannane in **21a** with carrier-free Na¹²⁵I in the presence of chloramine-T gave [¹²⁵I]**17a** (47–65 % radiochemical yield, 1–7 mCi scale, 96–99 % radiochemical purity).

Compound **17a** displayed an affinity for FKBP12 some two orders of magnitude lower than rapamycin (Table 1) but activity in the splenocyte assay was reduced to no greater an extent, suggesting that the affinity of the FKBP12–compound **17a** complex for the target protein was comparable to that of the rapamycin complex. An inactive rapamycin derivative, compound **22a**, was synthesized as a control by retroaldol cleavage [23] of the macrocyclic ring using ZnCl₂ in THF at room temperature (65 % yield, Fig. 5). Compound **22a** exhibited FKBP12 affinity similar to that of **17a** (K_i = 30 and 73 nM for **17a** and **22a**, respectively), but, lacking a functional effector domain, showed no significant activity in the splenocyte assay. Thus, we expected compounds **17a** and **22a** to interact similarly with FKBP family members, but to interact differently with the downstream target protein.

A major protein band of molecular mass ~250 kDa (p250) was strongly and reproducibly labeled by compound **17a**. This protein was strongly labeled in CTLL-20 extracts or whole cells, and was also present in Jurkat and THP-1 cells (Fig. 6). We were able to separate p250 from the majority of cytosolic FKBP by ultracentrifugation. Labeling of p250 was enhanced after addition of exogenous FKBP, suggesting that it is dependent on FKBP (Fig. 6).

The specificity of p250 labeling by **17a** was evaluated by competition experiments. Low levels of rapamycin abolished labeling, while higher concentrations produced high backgrounds (Fig. 7). We interpret this result as indicating the displacement of compound **17a** from FKBP by high concentrations of rapamycin, leading to loss of labeling specificity. FK506 at low concentrations failed to compete with **17a** for labeling of p250. Higher concentrations produced background labeling of proteins and reduced the p250 signal (Fig. 7). The inactive seco-derivative, **22a**, failed to compete at any concentration tested (Fig. 7).

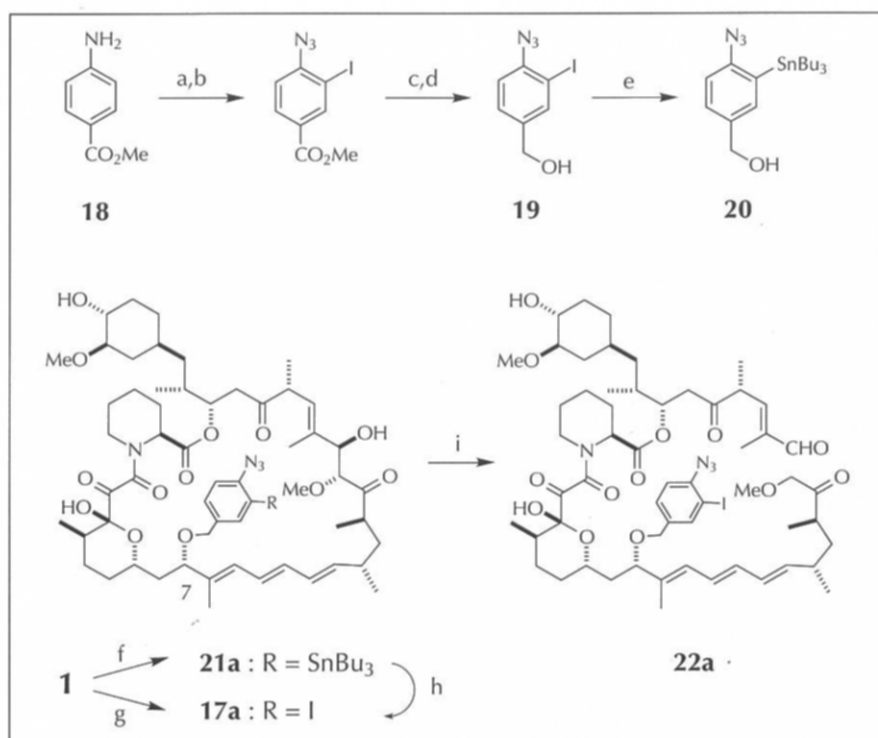


Fig. 5. Synthesis of the photoaffinity label reagents **17a** and **22a**. (a) N-iodosuccinimide (NIS), cat. H₂SO₄, MeCN, 67 %; (b) NaNO₂, conc HCl, then NaN₃, 95 %; (c) LiOH, MeOH; (d) isobutyl chloroformate, Et₃N, then NaBH₄, 62 % steps c–d; (e) (Bu₃Sn)₂, (Ph₃P)₂PdBr₂, toluene, dimethyl formamide (DMF), 100 °C, 62 %; (f) compound **19** (excess), *p*-TsOH, CH₂Cl₂, room temperature, 66 % of 1:1 C-7 epimers; (g) compound **20** (excess), *p*-TsOH, CH₂Cl₂, room temperature, 14 % of **21a**; (h) chloramine-T, Na¹²⁵I; (i) ZnCl₂, tetrahydrofuran (THF), room temperature, 65 %.

The results show that **17a** specifically labels a protein of 250 kDa that is present in all three cell lines examined, two of which are of T-cell origin and one that is monocyte-like. Labeling was dependent on FKBP12; rapamycin could compete for labeling, whereas FK506 and

compound **22a** could not. Compound **17a** does not label FKBP12 itself. These findings are consistent with a role for p250 as a downstream target for the rapamycin–FKBP12 complex. Western blotting with antiserum to FRAP showed that FRAP was present in our cell extracts (Fig. 8). Three other bands that cross-react with the antiserum to FRAP were also seen. We do not know what relationship, if any, these proteins have to FRAP, but imaging of radioactivity in photolabeled extracts showed that only one band was labeled by the photoaffinity reagent. This band co-migrated with recombinant FRAP, consistent with the possibility that compound **17a** is labeling FRAP.

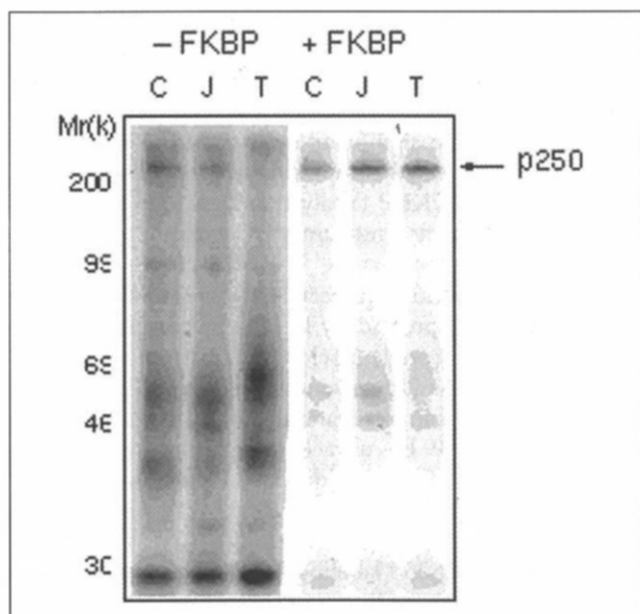
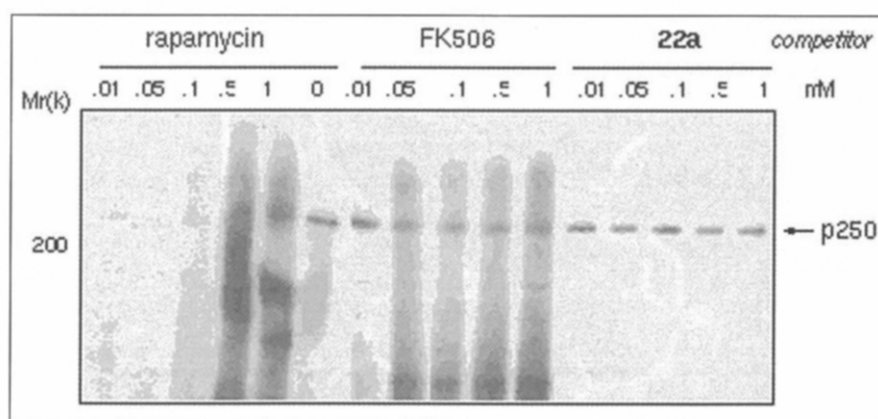


Fig. 6. FKBP12-dependent photoaffinity labeling of p250 by rapamycin derivative **17a**. CTLL-20 (C), Jurkat (J), and THP-1 (T) cell extracts were centrifuged at 130 000 × g and the pellets were washed to remove endogenous FKBP. Pellets were resuspended in PBS, incubated with 10 nM **17a** in the presence or absence of 10 μM FKBP12 for 30 min and irradiated with a Hg vapor UV lamp. Following gel filtration to remove unbound radiolabel, the protein fraction was electrophoresed on 10 % polyacrylamide gel and visualized by autoradiography.

Atomic models of selected FKBP12 complexes

Four C-7 rapamycin analogs (compounds **4**, **6a**, **6b** and **9**) complexed with FKBP12 were selected for detailed structural studies by single crystal X-ray diffraction. Compound **4** allowed the direct comparison of rapamycin and C-7 epirapamycin, while **6a** and **6b** provided an independent assessment of an epimeric pair with a modest increase in steric bulk. Compound **9** allowed the structural alterations induced by a bulky hydrophobic substituent to be studied. The protein components of all four complexes show the same folding topology found in the initial FKBP12–rapamycin structure [17], and as can be seen in Table 2, the root-mean square deviations for main chain atoms are 0.16, 0.13, 0.14 and 0.50 Å for compounds **4**, **6a**, **6b** and **9**, respectively. For the smaller C-7 substituents (in **4**, **6a**, and **6b**) the complexed ligands show no significant conformational differences from complexed rapamycin (Table 2), and the root-mean square deviations are 0.30, 0.17 and 0.55 Å. Not surprisingly, compound **6a** is closer to rapamycin than **6b** or **4**, but the overall picture is one of little conformational dependence on C-7 stereochemistry for the smaller substituents. The bound

Fig. 7. Competition for labeling of p250 by rapamycin, FK506 or seco-rapamycin derivative **22a**. Washed pellets from a 130 000 \times g spin of Jurkat extract were reconstituted with 0.5 μ M FKBP12 and preincubated with competitor at the indicated concentrations for 30 min before being irradiated in the presence of 10 nM rapamycin-derived photoaffinity label **17a**. Protein fractions were subjected to 6% SDS-PAGE and visualized by autoradiography.



conformations of these ligands do not appear to be especially sensitive to stereochemistry at C-7 (Fig. 9).

While the FKBP12 complexes with compounds **4**, **6a**, and **6b** were all isomorphous with rapamycin, the complex with compound **9** was not, and the bulky C-7 substituent resulted in different intermolecular interactions and different crystal packing. The crystal structure of FKBP12–compound **9** was complicated, with four molecules, #1, #2, #3 and #4, in the asymmetric unit. Two pairs of molecules, #1–#2 and #3–#4, were related by a noncrystallographic two-fold axis and had no significant differences, although the trimethoxyphenyl group of the #1–#2 pair showed some disorder. The differences between #1 and #3 were quantitative, not qualitative. Both #1 and #3 had significant main-chain deviations from the FKBP12–rapamycin structure in the regions centered on residue 33 and 88 (Fig. 9). The region centered on residue 33, which is not near the bound ligand, is on the surface of the protein and in the contact with other molecules and symmetry-related molecules. Thus the deviations probably result from the altered crystal packing and intermolecular interactions. The deviation in the region around residue 88 appears to be a direct result of the bulky substituent at C-7. Residue 88 is in the tip of the 80s loop, which is near the ligand binding site and known to be important in binding of FKBP12–FK506 to

calcineurin. The bulky trimethoxyphenyl substituent at C-7 forces the residues at the tip of the 80s loop to move away slightly from the ligand and is reflected in the changes seen in Table 2. The trimethoxyphenyl substituent also occupies the region of space thought to be crucial for FRAP binding and thus could account for the observed lack of cellular activity (Table 1).

Significance

Rapamycin, a potent and clinically important immunosuppressant, mediates a precise disruption of cell cycle progression in T-lymphocytes by inducing a protein–protein dimerization event. Rapamycin has two domains, one binding with nanomolar affinity to FKBP12, the other (the effector domain) forming a new binding surface when complexed with FKBP12, which allows binding to a recently identified 289-kDa protein of unknown function (FRAP). Synthetic modifications to the binding domains of rapamycin and the structurally related FKBP ligand FK506, along with X-ray crystallography, have provided some insight into the FKBP–rapamycin interaction. However, synthetic modifications to the rapamycin effector domain have been extremely limited. The remarkable reactivity of the C-7 methoxy group of rapamycin has allowed us to replace this group with a wide range of substituents.

Here we report that modifications to the C-7 center of rapamycin result in divergences between the biological effects of the rapamycin analogs and their ability to bind FKBP12. Thus, it is plausible that the C-7 substituent may form part of the FRAP-binding surface. Some groups of substantially greater steric demand than the methoxy group still allowed FRAP binding, suggesting that the C-7 substituent may lie in an interfacial space between FKBP12 and FRAP. The X-ray crystal structures of complexes of several of these analogs with FKBP12 show that the overall fold of the protein and the ligand conformation are essentially identical to those observed for the parent rapamycin bound to FKBP12.

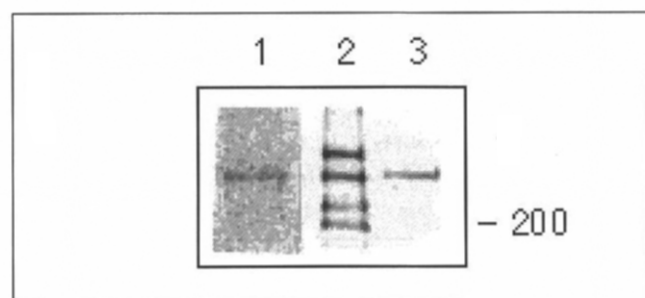


Fig. 8. The protein labeled by compound **17a** co-migrates with FRAP. Jurkat cell extract was photolabeled with rapamycin derivative **17a** and, following 7% SDS-PAGE, exposed on a phosphorimager screen to visualize radioactive proteins (lane 1). Jurkat extracts (lane 2) were subjected in parallel with recombinant FRAP (lane 3) to 7% SDS-PAGE and Western blotted with antiserum to FRAP.

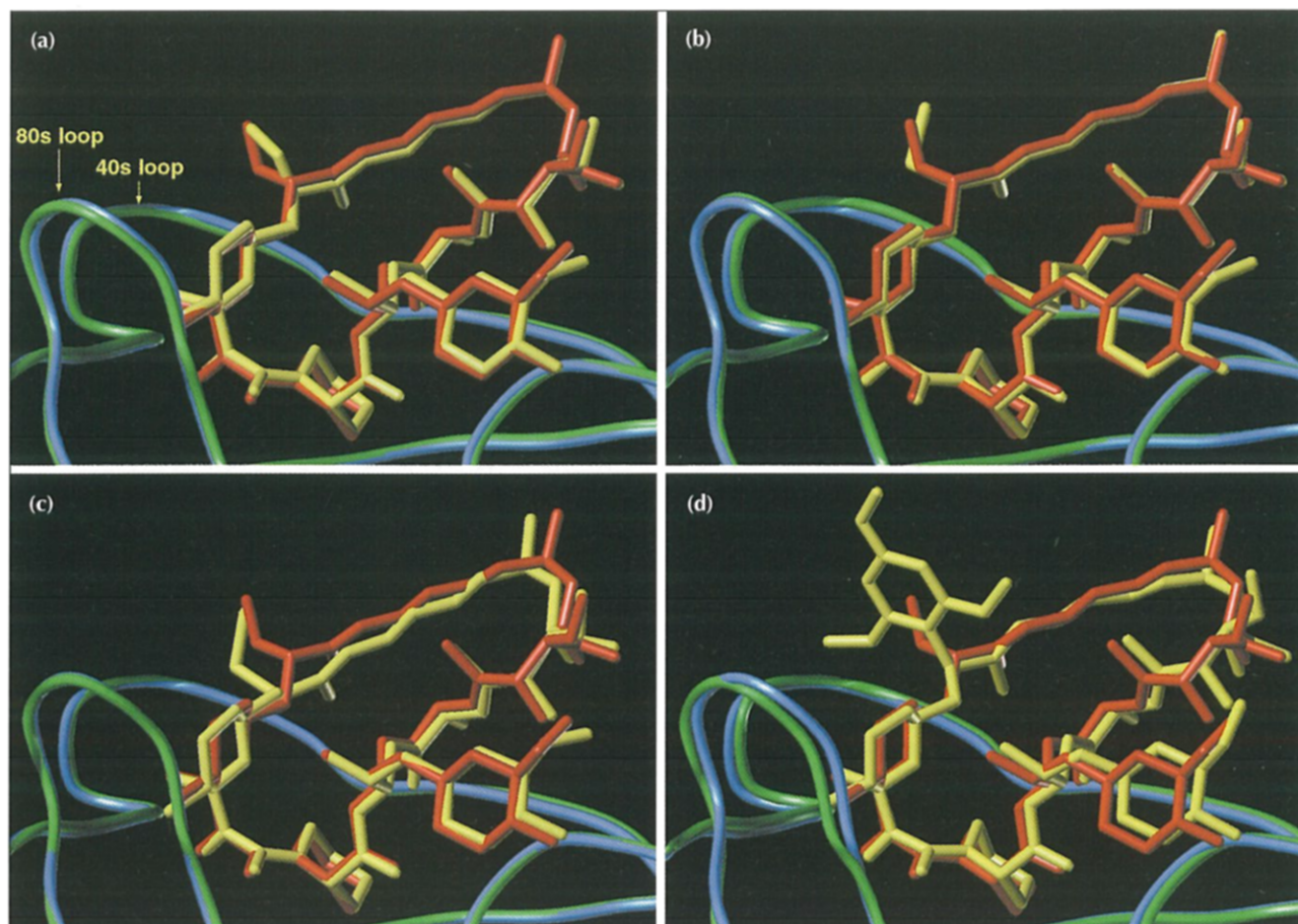


Fig. 9. Superimpositions of crystal structures of complexes of FKBP12 with rapamycin analogs. Superimpositions of (a) FKBP12–compound **4** (7-epi-rapamycin), (b) FKBP12–compound **6a** (7-thiomethyl), (c) FKBP12–compound **6b** (7-epi-thiomethyl) and (d) FKBP12–compound **9** (7-epi-trimethoxyphenyl, molecule #3 is shown) with FKBP12–rapamycin [14] are shown. Rapamycin is depicted as red; rapamycin derivatives are depicted as yellow. Proteins are shown as a backbone traces only (FKBP12 in complex with rapamycin: green, FKBP12 in complex with the analog (FKBP–X): blue). Structures were superimposed using a least-squares fit of protein backbone heavy atoms.

We have extended the application of this chemistry to introduce a photoreactive radiolabel into the C-7 position and demonstrated a selective, FKBP12-dependent labeling of a T-cell protein of apparent molecular mass 250 kDa, which may be FRAP. Further manipulation of the rapamycin effector domain, particularly at C-7, may yield rapamycin analogs with enhanced FRAP affinity and therefore greater therapeutic efficacy.

Materials and methods

Preparation of compounds **5a** and **5b**

To a solution of rapamycin (2.2 g, 2.41 mmol) in EtOH (100 ml) at room temperature was added *p*-TsOH (1.3 g, 12 mmol) and the reaction was monitored for disappearance of rapamycin. After 2 h, the mixture was diluted with EtOAc, and the organic extracts washed with saturated NaHCO₃, brine and dried over Na₂SO₄. The crude material was purified by preparative silica gel high-pressure liquid chromatography (HPLC; lichrosphere Si60 column; eluted with 42:42:15:2–4.5 Hex:CHCl₃:EtOAc:MeOH), to give compound **5a** as a white solid (0.46 g) along with a mixture of **5a**:**5b** (~1:1, 1.6 g,

93 % overall yield). This latter material was repurified by silica gel HPLC to provide **5a** (760 mg) along with **5b** (785 mg). Data for **5a**: ¹H NMR (CDCl₃, 400 MHz, 4:1 mixture of *trans/cis* amide rotamers; data for the *trans*-rotamer): δ 6.375 (dd, *J* = 14.8, 10.3 Hz, 1 H, H-4), 6.300 (dd, *J* = 14.8, 9.6 Hz, 1 H, H-3), 6.134 (dd, *J* = 14.9, 9.6 Hz, 1 H, H-2), 5.940 (d, *J* = 10.3 Hz, 1 H, H-5), 5.533 (dd, *J* = 14.9, 9.2 Hz, 1 H, H-1), 5.408 (d, *J* = 9.7 Hz, 1 H, H-26), 5.29 (m, 1 H, H-20), 5.17 (m, 1 H, H-22), 4.799 (s, 1 H, OH-13), 4.173 (d, *J* = 5.9 Hz, 1 H, H-28), 3.87 (m, 1 H, H-9), 3.775 (dd, *J* = 7.8, 7.0 Hz, 1 H, H-7), 3.714 (d, *J* = 5.9 Hz, 1 H, H-29), 3.576 (br d, *J* = 14.0 Hz, 1 H, H-16), 3.407 (s, 3 H), 3.338 (s, 3 H), 3.161 (dq,

Table 2. Root-mean-square deviations of FKBP12–X structures from the FKBP12–rapamycin structure (Å).

X:	4	6a	6b	9 (#1)	9 (#3)
Main chain	0.16	0.13	0.14	0.54	0.45
Side chain	0.50	0.39	0.39	1.09	0.84
Ligand	0.30	0.17	0.55	2.21	1.06
All atoms	0.42	0.33	0.33	0.96	0.75

$J = 9.8, 6.9$ Hz, 1 H), 2.587 (dd, $J = 17.0, 6.3$ Hz, 1 H, H-23), 1.751 (s, 3 H), 1.662 (s, 3 H), 1.152 (t, $J = 6.9$ Hz, 3 H), 1.098 (d, $J = 6.7$ Hz, 3 H), 1.047 (d, $J = 6.5$ Hz, 3 H), 0.991 (d, $J = 6.6$ Hz, 3 H), 0.951 (d, $J = 6.6$ Hz, 3 H), 0.917 (d, $J = 6.7$ Hz, 3 H), 0.668 (q, $J = 12.0$ Hz, 1 H, H-41); ^{13}C NMR (CDCl_3 , 100.6 MHz, data for the *trans*-rotamer): δ 215.5, 208.2, 192.6, 169.3, 166.7, 140.0, 136.4, 136.0, 133.4, 130.2, 129.0, 126.7, 126.5, 98.5, 84.7, 84.4, 82.4, 77.2, 75.6, 73.9, 67.2, 63.3, 59.4; MS ($\text{ESI}^+/\text{NH}_4\text{OAc}$) m/z 950 ($\text{M}+\text{Na}^+$), 945 ($\text{M}+\text{NH}_4^+$); UV (MeOH) λ_{max} 267, 277, 289 nm. Data for **5b**: ^1H NMR (CDCl_3 , 400 MHz, 2.5:1 mixture of *trans*:*cis* amide rotamers; data for the *trans*-rotamer): δ 6.365 (dd, $J = 14.2, 11.0$ Hz, 1 H, H-4), 6.185 (dd, $J = 14.2, 10.4$ Hz, 1 H, H-3), 6.12–6.05 (m, 2 H, H-2 and H-5), 5.471 (dd, $J = 14.4, 9.1$ Hz, 1 H, H-1), 5.421 (d, $J = 10.3$ Hz, 1 H, H-26), 5.25–5.20 (m, 2 H, H-22 and H-20), 4.260 (br s, 1 H, H-28), 4.10–4.04 (m, 1 H, H-9), 4.050 (s, 1 H, OH-13), 4.012 (d, $J = 3.6$ Hz, 1 H, H-29), 3.698 (dd, $J = 8.1, 1.5$ Hz, 1 H, H-7), 3.50–3.41 (m, 2 H, H-16 and H from $\text{C}_7\text{-OEt}$), 3.394 (s, 3 H), 3.332 (s, 3 H), 3.232 (dt, $J = 13.4, 7.0$ Hz, 1 H, H from $\text{C}_7\text{-OEt}$), 2.718 (dd, $J = 17.4, 2.7$ Hz, 1 H, H-23), 2.376 (dd, $J = 17.4, 8.5$ Hz, 1 H, H-23), 1.750 (s, 3 H), 1.654 (s, 3 H), 1.180 (t, $J = 7.0$ Hz, 3 H), 1.059 (d, $J = 6.7$ Hz, 3 H), 1.005 (d, $J = 6.6$ Hz, 3 H), 0.941 (d, $J = 6.5$ Hz, 3 H), 0.925 (d, $J = 6.5$ Hz, 3 H), 0.863 (d, $J = 6.6$ Hz, 3 H), 0.646 (q, $J = 12.0$ Hz, 1 H, H-41); MS ($\text{ESI}^+/\text{NH}_4\text{OAc}$) m/z 950 ($\text{M}+\text{Na}^+$), 945 ($\text{M}+\text{NH}_4^+$).

Preparation of compounds **10a** and **10b**

To a solution of rapamycin (1.2 g, 1.31 mmol) and furan (3.8 ml, 52 mmol) in CH_2Cl_2 (52 ml) at -40°C was added trifluoroacetic acid (1.7 ml, 22 mmol), and the solution was stirred for 3 h at -40°C . The reaction mixture was then partitioned between EtOAc and brine. The organic extracts were dried with Na_2SO_4 , filtered, concentrated *in vacuo* and purified by chromatography (silica gel; elution with 200:50:42.5:7.5 CH_2Cl_2 :Hex:EtOAc:MeOH), to yield **10a** (740 mg, 59 %) and **10b** (380 mg, 30 %). Data for **10a**: ^1H NMR (CDCl_3 , 400 MHz, 4:1 mixture of *trans*:*cis* amide rotamers; data for the *trans*-rotamer): δ 7.290 (d, $J = 1.6$ Hz, 1 H, Ar H-5'), 6.39–6.32 (m, 2 H, H-4 and H-3), 6.289 (dd, $J = 3.2, 1.6$ Hz, 1 H, Ar H-4'), 6.16–6.11 (m, 1 H, H-2), 6.02–6.00 (m, 1 H, H-5), 6.006 (d, $J = 3.2$ Hz, 1 H, Ar H-3'), 5.615 (dd, $J = 15.1, 8.2$ Hz, 1 H, H-1), 5.424 (d, $J = 9.8$ Hz, 1 H, H-26), 5.336 (d, $J = 4.9$ Hz, 1 H, H-20), 5.191 (q, $J = 5.5$ Hz, 1 H, H-22), 5.096 (s, 1 H, OH-13), 4.200 (d, $J = 6.0$ Hz, 1 H, H-28), 3.85–3.90 (m, 1 H, H-9), 3.734 (d, $J = 6.0$ Hz, 1 H, H-29), 3.697 (dd, $J = 8.5, 8.1$ Hz, 1 H, H-7), 3.408 (s, 3 H), 3.357 (s, 3 H), 2.944 (ddd, $J = 11.3, 8.5, 4.1$ Hz, 1 H, H-42), 2.689 (d, $J = 6.2$ Hz, 2 H, H-23), 1.775 (s, 3 H), 1.559 (s, 3 H), 1.136 (d, $J = 6.8$ Hz, 3 H), 1.051 (d, $J = 6.6$ Hz, 3 H), 1.006 (d, $J = 6.5$ Hz, 3 H), 0.990 (d, $J = 6.5$ Hz, 3 H), 0.929 (d, $J = 6.8$ Hz, 3 H), 0.669 (q, $J = 12.0$ Hz, 1 H, H-41); ^{13}C NMR (CDCl_3 , 100.6 MHz, data for the *trans*-rotamer) δ 215.3, 208.7, 191.7, 169.2, 166.9, 156.8, 141.1, 138.9, 136.2, 135.5, 132.8, 129.9, 128.7, 126.9, 126.5, 109.9, 104.8, 98.2, 84.6, 84.3, 76.0, 73.8, 66.7; MS ($\text{ESI}^+/\text{NH}_4\text{OAc}$) m/z 967 ($\text{M}+\text{NH}_4^+$), 932. Data for compound **10b**: ^1H NMR (CDCl_3 , 400 MHz, 3.5:1 mixture of *trans*:*cis* amide rotamers; data for the *trans*-rotamer): δ 7.302 (d, $J = 1.8$ Hz, 1 H, Ar H-5'), 6.356 (dd, $J = 14.6, 10.9$ Hz, 1 H, H-4), 6.292 (dd, $J = 3.0, 1.8$ Hz, 1 H, Ar H-4'), 6.190 (dd, $J = 14.6, 10.4$ Hz, 1 H, H-3), 6.044 (br d, $J = 10.9$ Hz, 1 H, H-5), 6.019 (d, $J = 3.0$ Hz, 1 H, Ar H-3'), 5.390 (d, $J = 10.3$ Hz, 1 H, H-26), 5.327 (dd, $J = 14.7, 9.4$ Hz, 1 H, H-1), 5.24–5.09 (m, 2 H, H-22 and H-20), 4.294 (br s, H-28), 4.116 (d, $J = 3.1$ Hz, 1 H, H-29), 3.805 (s, 1 H, OH-13), 3.78–3.72 (m, 1 H, H-9), 3.524 (br d, $J =$

$J = 15.0$ Hz, 1 H, H-16), 3.469 (dd, $J = 11.7, 3.6$ Hz, 1 H, H-7), 3.391 (s, 3 H), 3.335 (s, 3 H), 3.245 (dq, $J = 10.3$ (d), 6.6 Hz, 1 H, H-25), 2.94–2.89 (m, 1 H, H-42), 2.763 (dd, $J = 17.7, 2.8$ Hz, 1 H, H-23), 2.360 (dd, $J = 17.7, 8.4$ Hz, 1 H, H-23), 1.825 (s, 3 H), 1.662 (s, 3 H), 1.058 (d, $J = 6.4$ Hz, 3 H), 0.973 (d, $J = 6.5$ Hz, 3 H), 0.924 (d, $J = 6.4$ Hz, 3 H), 0.888 (d, $J = 6.4$ Hz, 3 H), 0.883 (d, $J = 6.5$ Hz, 3 H), 0.633 (q, $J = 11.6$ Hz, 1 H, H-41); ^{13}C NMR (CDCl_3 , 100.6 MHz, data for the *trans*-rotamer) δ 211.0, 207.2, 196.3, 169.6, 166.0, 155.4, 141.5, 140.0, 137.8, 134.5, 131.2, 128.3, 125.6, 123.8, 110.1, 106.3, 98.5, 84.3, 83.7, 76.3, 73.9, 73.8, 68.3; MS ($\text{ESI}^+/\text{NH}_4\text{OAc}$) m/z 972 ($\text{M}+\text{Na}^+$), 967 ($\text{M}+\text{NH}_4^+$).

Preparation of compound **13**

To a solution of rapamycin (50 mg, 0.055 mmol) in CH_2Cl_2 (1 ml) at 0°C was added water (0.2 ml) followed by 2,3-dichloro-5,6-dicyano-1,4-benzoquinone (DDQ) (25 mg, 0.109 mmol). After 2 min the reaction is complete by thin-layer chromatography and the mixture was partitioned between EtOAc and saturated NaHCO_3 (0.5 ml). Purification by silica gel chromatography afforded compound **13** (32 mg, 65 %). ^1H NMR (CDCl_3 , 400 MHz, 3:1 mixture of *trans*:*cis* amide rotamers; data for the *trans*-rotamer): δ 7.146 (d, $J = 10.8$ Hz, 1 H, H-5), 6.633 (dd, $J = 14.9, 10.6$ Hz, 1 H, H-3), 6.498 (dd, $J = 14.9, 10.8$ Hz, 1 H, H-4), 6.224 (dd, $J = 15.1, 10.6$ Hz, 1 H, H-2), 5.660 (dd, $J = 15.1, 9.3$ Hz, 1 H, H-1), 5.443 (d, $J = 9.9$ Hz, 1 H, H-26), 5.25–5.20 (m, 1 H, H-22), 5.151 (d, $J = 4.6$ Hz, 1 H, H-20), 4.820 (s, OH-13), 4.53–4.47 (m, 1 H, H-9), 4.305 (br d, $J = 4.7$ Hz, 1 H, H-28), 3.990 (d, $J = 4.7$ Hz, 1 H, H-29), 3.387 (s, 3 H), 3.349 (s, 3 H), 3.223 (dd, $J = 15.4, 9.0$ Hz, 1 H, H-8), 2.94–2.88 (m, 1 H, H-42), 2.462 (dd, $J = 15.4, 3.7$ Hz, 1 H, H-8), 1.862 (s, 3 H), 1.804 (s, 3 H), 1.080 (d, $J = 6.5$ Hz, 3 H), 1.027 (d, $J = 6.8$ Hz, 3 H), 0.980 (d, $J = 6.6$ Hz, 3 H), 0.934 (d, $J = 6.7$ Hz, 3 H), 0.847 (d, $J = 6.6$ Hz, 3 H), 0.655 (q, $J = 11.7$ Hz, 1 H, H-41); ^{13}C NMR (CDCl_3 , 100.6 MHz, data for the *trans*-rotamer): δ 212.5, 208.1, 199.5, 197.7, 169.2, 166.6, 143.6, 139.8, 139.1, 136.7, 135.9, 130.5, 127.3, 125.8, 99.0, 85.2, 84.4, 84.3, 77.2, 76.4, 74.7, 73.9, 68.1; MS ($\text{ESI}^+/\text{NH}_4\text{OAc}$) m/z 920 ($\text{M}+\text{Na}^+$), 915 ($\text{M}+\text{NH}_4^+$), 898, 880; UV (MeOH) λ_{max} 318 nm.

FKBP12 assays

Apparent rotamase inhibition constants, $K_{i,\text{app}}$, were determined using the chymotrypsin-coupled assay previously reported [18] and are used here as an approximate measure of ligand binding affinities.

Splenocyte proliferation assays

Spleen cells from BDF1 female mice were established in RPMI with 10 % fetal calf serum at $5 \times 10^6 \text{ ml}^{-1}$. One hundred μl aliquots of this suspension (5×10^5 cells) were dispensed into 96-well round-bottomed microtiter plates (Linbro, Flow Laboratories). Concanavalin A ($5 \mu\text{g ml}^{-1}$) was added as the mitogenic stimulus and the final volume in the microtiter wells was adjusted to 200 μl with RPMI. Cell cultures were incubated for 72 h at 37°C in a 5 % CO_2 atmosphere and pulsed with 0.5 μCi ^3H -thymidine (specific activity 2.00 Ci mmol^{-1}) for the last 18 h of the 72 h culture. The cells were harvested on an automated multiple sample harvester and cell-associated radioactivity counted in a Beckman liquid scintillation counter. The results are expressed as the mean values derived from quadruplicate measurements. Cell viability was determined by trypan blue exclusion after 72 h of incubation. Compounds to be tested were added to the microtiter plates at the appropriate dilutions prior to the addition of cells.

Yeast assays

A standard agar diffusion assay was used to measure the yeast cytotoxicity of the compounds. 2×10^7 yeast cells were plated on 25 x 25 cm YEPD plates and wells were made in the agar. One hundred μ l of compound solutions of various concentrations (dissolved in 1:1 DMSO:MeOH) were added to the wells. After 48 h of incubation at 30 °C the zones of inhibition of growth were measured. Linear regression analysis was applied to plots of zone diameters versus the log of concentration of compounds to obtain IC_{12} values. IC_{12} is defined as the concentration of compounds in the well that would give a 12-mm zone of inhibition.

Crystallization and data collection

Recombinant human FKBP12 purified from *Escherichia coli* was used at 10 mg ml⁻¹ in 10 mM Tris-HCl, pH 8.0. The four selected rapamycin analogs were dissolved in methanol and mixed with FKBP12 at a 2:1 molar ratio. The mixture was lightly vortexed, allowed to stand overnight to complete complex formation, and filtered. All crystallizations were done using the hanging drop method. Crystals of compounds **4**, **6a** and **6b** complexed with FKBP12 were obtained under slightly different conditions from those of the rFKBP12-rapamycin complex crystal (Table 3). Both micro- and macro-seeding techniques were used to improve the crystal size and quality. After 1 to 3 weeks, rectangular rod-like crystals with a maximum size of 0.5 x 0.4 x 0.2 mm, which were suitable for data collection, were obtained. Crystals of the FKBP12-compound **9** complex were obtained under very different conditions (Table 3). Trigonal plate-shaped crystals with dimensions of 0.4 x 0.3 x 0.1 mm were obtained in about 2 months.

All four data sets were collected at room temperature on a San Diego multiwire area detector system mounted on a Rigaku RU-200 rotating anode X-ray source operating at 50 kV x 130 mA. Crystals of the complexes with compounds **4**, **6a** and **6b** were isomorphous with FKBP12-rapamycin, and formed in the orthorhombic space group $P2_12_12_1$ with one molecule in the asymmetric unit. The FKBP12-compound **9** complex crystallized in the monoclinic space group $P2_1$ with four molecules in the asymmetric unit.

Structure determination and refinement

The structure determination of the complexes with compounds **4**, **6a** and **6b** was quite straightforward. Difference electron density maps were calculated using observed structure factors, calculated structure factors of FKBP12-rapamycin and FKBP12-rapamycin phases. The difference electron density maps were displayed with CHAIN [24]. The $F_o - F_c$ maps showed positive and negative peaks around the C-7 position that were consistent with the modifications expected. Based on these maps, models were constructed and refined with the X-PLOR package [25].

Crystallographic parameters and refinement statistics are shown in Table 4.

The structure of the FKBP12-compound **9** complex was determined using molecular replacement. The complex contained four molecules in the asymmetric unit and a self rotation map showed that there are two non-crystallographic two-fold axes. The cross rotation search using the rapamycin-FKBP12 structure as a model revealed four clear peaks. Two peaks are related by a two-fold axis and the other two peaks are also related by a two-fold axis; these two pairs are related by a 90° rotation. The translation search was performed for each of the cross rotation solutions, and gave an unambiguous solution for each solution. Rigid body refinement led to an R-factor of 0.345 (8-3 Å). The structure was refined with X-PLOR using noncrystallographic symmetry restraints [25]. Final refinement statistics are shown in Table 4.

Photoaffinity labeling

Cell lines were obtained from the American Type Culture Collection. All cell lines were cultured in suspension in RPMI 1640 medium plus 10 % fetal bovine serum and were regularly screened for mycoplasma contamination. Cells were incubated in 75 mM KCl, 10 mM HEPES pH 7.9, 0.25 M sucrose, 0.1 mM EDTA, 0.1 mM EGTA, 0.5 mM PMSF, 1 μ g ml⁻¹ pepstatin and leupeptin) for 15 min at 0 °C. NP40 was added to 0.1 % final concentration to lyse the plasma membranes but not the nuclei. Extracts were centrifuged at 200 x g for 5 min and at 130 000 x g for 30 min. The pellet from this step was resuspended in 0.15 M NaCl, 0.1 M NaH₂PO₄, 10 mM Na₂HPO₄ pH 7.4 (PBS) and incubated with 10 nM radiophotoaffinity label, **17a**, in the presence or absence of 10 μ M recombinant FKBP12 and competitor compounds at room temperature for 30 min under subdued lighting. Samples were irradiated for 5 min on ice under a 500W mercury vapor UV source. Bound label was separated from free by gel filtration chromatography on a Sephadex G50 spin column presaturated with bovine serum albumin. Laemmli sample buffer was added to the protein fraction and run without boiling on 6-10 % polyacrylamide gels. Radioactive bands were visualized by autoradiography.

Western blotting

Cell extracts were run in parallel with recombinant FRAP on a 7 % reducing SDS-polyacrylamide gel and proteins were transferred to nitrocellulose. Following a block with 5 % Carnation milk/PBS/0.5 % Tween-20, the blot was probed for 1 h with a 2 μ g ml⁻¹ solution of affinity-purified (synthetic FRAP peptide) rabbit polyclonal antisera. The blot was washed with PBS/0.5 % Tween-20 and probed for 1 h with a 1:5000 dilution of peroxidase-conjugated goat anti-rabbit antibody. Following a wash with PBS/0.5 % Tween-20, the blot was developed with ECL reagent and exposed to film for 30 s. The same cell extract was photolabeled and run on a 7 % gel as

Table 3. Crystallization conditions for selected FKBP12 complexes.

Rapamycin (1)	Compound 4	Compound 6a	Compound 6b	Compound 9
0.1 M phosphate (pH 6.0)	0.1 M phosphate (pH 5.9)	0.1 M phosphate (pH 5.9)	0.1 M Na acetate (pH 4.6)	2.0 M ammonium sulfate
0.4 M ammonium sulfate	2.5 M ammonium sulfate	0.3 M ammonium sulfate	2.7 M ammonium sulfate	5 % isopropanol

Table 4. Crystallographic parameters and refinement statistics.

	Compound 4	Compound 6a	Compound 6b	Compound 9
Space group	P2 ₁ 2 ₁ 2 ₁	P2 ₁ 2 ₁ 2 ₁	P2 ₁ 2 ₁ 2 ₁	P2 ₁
Lattice parameters	a = 45.16 Å b = 49.37 Å c = 54.57 Å	a = 45.45 Å b = 49.40 Å c = 54.88 Å	a = 45.28 Å b = 49.22 Å c = 54.49 Å	a = 51.34 Å b = 90.83 Å c = 51.36 Å b = 90.25 °
No. of complexes per asymmetric unit	1	1	1	4
Refinement statistics				
R factor	0.183	0.180	0.174	0.183
R _{free}	0.206	0.204	0.188	0.216
Resolution (Å)	8.0–2.3	8.0–2.1	8.0–2.1	8.0–2.8
RMS for bond distance (Å)	0.007	0.007	0.007	0.009
RMS for bond angle (°)	1.4	1.5	1.4	1.7
RMS for improper torsion angle (°)	1.8	1.8	1.8	2.2
No. of water molecules	70	61	73	–
Average B-factor for main chain (Å ²)	19.4	19.8	15.5	7.52
Average B-factor for all atoms (Å ²)	22.5	22.7	18.9	9.02

above and exposed on a phosphorimaging screen to visualize radiolabeled proteins.

Acknowledgements: We are grateful to Jie Chen and Professor Stuart Schreiber (Harvard University and Howard Hughes Medical Institute) for supplying recombinant FRAP and FRAP antiserum, and to the Analytical Chemistry Department, SmithKline Beecham for the determination of mass spectra.

References

- Morris, R.E. (1992). Rapamycins: antifungal, antitumor, antiproliferative, and immunosuppressive macrolides. *Transplant. Rev.* **6**, 39–87.
- Sehgal, S.N., Molnar-Kimber, K., Ocain, T.D. & Weichman, B.M. (1994). Rapamycin: a novel immunosuppressive macrolide. *Med. Res. Rev.* **14**, 1–22.
- Austin, D.J., Crabtree, G.R. & Schreiber, S.L. (1994). Proximity versus allostery: the role of regulated protein dimerization in biology. *Chemistry & Biology* **1**, 131–136.
- Schreiber, S.L. (1991). Chemistry and biology of the immunophilins and their immunosuppressive ligands. *Science* **251**, 283–287.
- Rosen, M.K. & Schreiber, S.L. (1992). Natural products as probes of cellular function: studies of immunophilins. *Angew. Chem. Int. Ed. Engl.* **31**, 384–400.
- Fruman, D.A., Burakoff, S.J. & Bierer, B.E. (1994). Immunophilins in protein folding and immunosuppression. *FASEB J.* **8**, 391–400.
- Liu, J., Farmer, J.D. Jr, Lane, W.S., Friedman, J., Weissman, I. & Schreiber, S.L. (1991). Calcineurin is a common target of cyclophilin-cyclosporin A and FKBP-FK506 complexes. *Cell* **66**, 807–815.
- Brown, E.J., *et al.*, & Schreiber, S.L. (1994). A mammalian protein targeted by G1-arresting rapamycin-receptor complex. *Nature* **369**, 756–758.
- Sabatini, D.M., Erdjument-Bromage, H., Lui, M., Tempst, P. & Snyder, S.H. (1994). RAFT1: a mammalian protein that binds to FKBP12 in a rapamycin-dependent fashion and is homologous to yeast TORs. *Cell* **78**, 35–43.
- Chiu, M.L., Katz, H. & Berlin, V. (1994). RAPT1, a mammalian homolog of yeast Tor, interacts with the FKBP12/rapamycin complex. *Proc. Natl. Acad. Sci. USA* **91**, 12574–12578.
- Chen, Y., *et al.*, & Molnar-Kimber, K.L. (1994). A putative sirolimus (rapamycin) effector protein. *Biochem. Biophys. Res. Commun.* **203**, 1–7.
- Kunz, J., Henriquez, R., Schneider, U., Deuter-Reinhard, M., Mowva, N.R. & Hall, M.N. (1993). Target of rapamycin in yeast, TOR2, is an essential phosphatidylinositol kinase homolog required for G₁ progression. *Cell* **73**, 585–596.
- Cafferkey, R., *et al.*, & Livi, G.P. (1993). Dominant missense mutations in a novel yeast protein related to mammalian phosphatidylinositol 3-kinase and VPS34 abrogate rapamycin cytotoxicity. *Mol. Cell. Biol.* **13**, 6012–6023.
- Van Duyn, G.D., Standaert, R.F., Karplus, P.A., Schreiber, S.L. & Clardy J. (1993). Atomic structures of the human immunophilin FKBP-12 complexes with FK506 and rapamycin. *J. Mol. Biol.* **229**, 105–124.
- Aldape, R.A., Futer, O., DeCenzo, M.T., Jarrett, B.P., Murcko, M.A. & Livingston, D.J. (1992). Charged surface residues of FKBP12 participate in formation of the FKBP12–FK506–calcineurin complex. *J. Biol. Chem.* **267**, 16029–16032.
- Yang, D., Rosen, M.K. & Schreiber, S.L. (1993). A composite FKBP12–FK506 surface that contacts calcineurin. *J. Am. Chem. Soc.* **115**, 819–820.
- Luengo, J.L., Konialian-Beck, A., Rozamus, L.W. & Holt, D.A. (1994). Manipulation of the rapamycin effector domain. Selective nucleophilic substitution of the C₇ methoxy group. *J. Org. Chem.* **59**, 6512–6513.
- Holt, D.A., *et al.*, & Clardy, J. (1993). Design, synthesis, and kinetic evaluation of high-affinity FKBP ligands and the X-ray crystal structures of their complexes with FKBP12. *J. Am. Chem. Soc.* **115**, 9925–9938.
- Liu, J., *et al.*, & Schreiber, S.L. (1992). Inhibition of T cell signaling by immunophilin–ligand complexes correlates with loss of calcineurin phosphatase activity. *Biochemistry* **31**, 3896–3901.
- Koltin, Y. & Livi, G.P. (1991). Rapamycin sensitivity in *Saccharomyces cerevisiae* is mediated by a peptidyl-prolyl *cis*–*trans* isomerase related to human FK506-binding protein. *Mol. Cell. Biol.* **11**, 1718–1723.
- Foor, F., *et al.*, & Nielsen, J.B. (1992). Calcineurin mediates inhibition by FK506 and cyclosporin of recovery from α -factor arrest in yeast. *Nature* **360**, 682–684.
- Rotonda, J., Burbaum, J.J., Chan, H.K., Marcy, A.I. & Becker, J.W. (1993). Improved calcineurin inhibition by yeast FKBP12–drug complexes. *J. Biol. Chem.* **268**, 7607–7609.
- Luengo, J.L., Konialian, A.L. & Holt, D.A. (1993). Studies on the chemistry of rapamycin: novel transformations under Lewis–acid catalysis. *Tetrahedron Lett.* **34**, 991–994.
- Sack, J.S. (1988). CHAIN — A crystallographic modeling program. *J. Mol. Graph.* **6**, 224–225.
- Brünger, A.T. (1992). *X-PLOR Manual, version 3.1*. Yale University Press, New Haven.

Received: 30 Jun 1995. Accepted: 5 Jul 1995.